Heme-catalases

Maria J Maté, Garib Murshudov, Jerónimo Bravo, William Melik-Adamyan, Peter C Loewen and Ignacio Fita

in

Handbook of Metalloproteins

Edited by

Albrecht Messerschmidt, Robert Huber, Thomas Poulos and Karl Wieghardt

Heme-catalases

Maria J Maté[†], *Garib Murshudov*[‡], *Jerónimo Bravo*[†], *William Melik-Adamyan*[§], *Peter C Loewen*[¶] *and Ignacio Fita*[†]

[†]IBMB (C.S.I.C.), Jordi Girona 18-26, 08034 Barcelona, Spain
[‡]Department of Chemistry, University of York, YO1 5DD York, United Kingdom
[§]Institute of Crystallography, Russian Academy of Sciences, 117333 Moscow, Russia
[¶]Department of Microbiology, University of Manitoba, R3T 2N2 Winnipeg, Canada

FUNCTIONAL CLASS

Enzyme; hydrogen peroxide: hydrogen peroxide oxidoreductase; EC 1.11.1.6.

Catalases can be considered as peroxidases specialized in the dismutation of hydrogen peroxide to oxygen and water, *the catalatic reaction*, according to the overall exothermic process (Equation (1)):

$$2H_2O_2 \rightarrow 2H_2O + O_2 \qquad (1)$$

Four categories of enzymes with catalase activity, three of them corresponding to well characterized unrelated gene families, have been defined:

(a) The classic mono-functional heme-containing tetrameric enzymes in either large or small subunit variations. This is the widest and most extensively studied, particularly at the structural level, group of catalases.[1,2]
(b) The non-heme, Manganese-containing catalases, which have been reported only in prokaryotes.[3–5]
(c) The heme-containing catalase-peroxidases, which are widely distributed among prokaryotes and also found in lower eukaryotes.[6,7]
(d) Finally a group of miscellaneous heme-containing enzymes, with secondary reactions in the form of low levels of catalatic activity, that include methemoglobin, metmyoglobin and the chloroperoxidase from *Caldariomyces fumago*.[8]

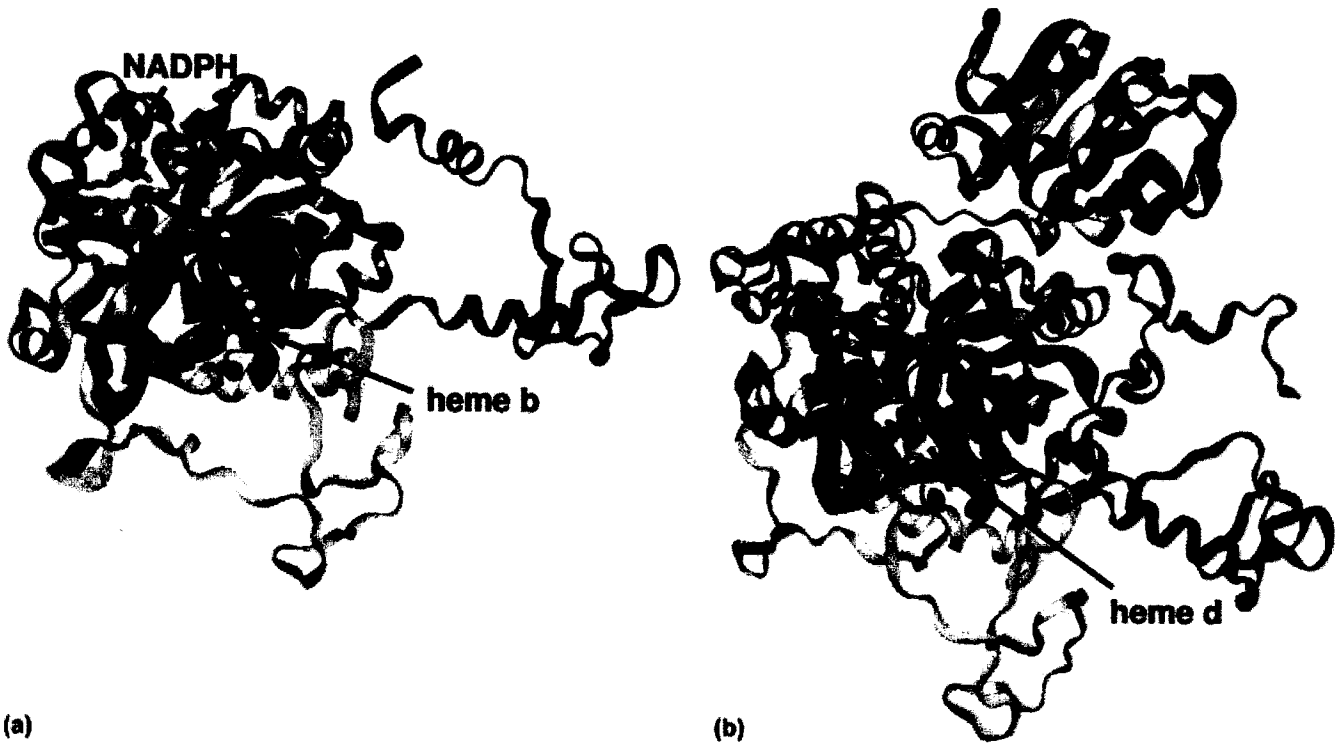

3D Structure Ribbon drawings of catalase structures corresponding to (a) beef liver (BLC; PDB code: 7CAT) and (b) HPII from *Escherichia coli* (PDB code 1IPH) as representative members of the small and the large subunit size enzymes respectively. The location of heme cofactors in the two structures and of NADP(H) in BLC are explicitly indicated. The four molecular regions defined in the small subunit size catalases, and the five regions in the large subunit size catalases (see text), are represented with different colors.

Catalase has been the subject of interest throughout the twentieth century, with the biochemical characterization and naming of the enzyme appearing first in 1900.[9] A number of reviews dealing with the physiology, biochemistry and structure of heme-catalases are available[1,7,8,10–14] and even the history of the studies about catalases has been analyzed.[2] The present work will focus on the structure of mono-functional heme-catalases, emphasizing the information obtained in the last few years mainly in relation to the catalytic functioning of these enzymes.

OCCURRENCE

Catalases are ubiquitous enzymes present in practically all aerobic prokaryote and eukaryote organisms and even in some facultative anaerobes.[15] In eukaryotic cells, catalase is located in the cytosol, but also in the mitochondria[8,16] and, particularly, in the peroxisomes, which are cellular organelles specialized in a number of oxidative processes that can result in the generation of hydrogen peroxide such as the β-oxidation of long chain fatty acids.[12] Numerous organisms present a number of catalase isozymes encoded by multiple genes, as initially reported for plants.[8,17] In turn, in most mammals catalase appears to be the product of a single structural gene, though various amounts of sialic acid attached to the enzyme or other postranscriptional modifications may give rise to the frequently observed heterogeneity.[18,19] Mammal catalases also present a widely variable tissue distribution with large concentrations of the enzyme found in liver, kidney, erythrocytes and marrow bone.[20]

BIOLOGICAL FUNCTION

Although the whole range of biological functions of catalases remains uncertain, the primary role appears to be the removal of small peroxides, particularly hydrogen peroxide, before they can cause cellular damage either directly or through their reactive breakdown products such as the highly reactive oxidant, the hydroxyl radical. Consistent with this protective role, catalase levels generally respond to oxidative stress, but with many species-specific variations. Among the prokaryotes, oxidative stress responses are often part of more general stress responses to temperature, salinity or starvation.[13] Among the eukaryotes, developmental changes, general metabolic changes, pathogenesis, radiation, hormones, temperature extremes, extreme oxygen concentrations and hydrogen peroxide have all been observed to influence catalase levels.[8] Besides that primary protective role the catalase system can also have a considerable physiological significance in biological oxidations, such as the metabolization of methanol and ethanol, in a number of living organisms.[21,22] Under physiological conditions catalase may also play a role in the compartmentalization of hydrogen peroxide,[23] a molecule that is gaining attention in signaling as a potential second messenger.[24,25]

The physiology of the catalase expression in various organisms has been extensively reviewed.[7,8,13]

AMINO ACID SEQUENCE INFORMATION

There are currently 120 catalase sequences reported and comparison reveals a strong sequence homology for about 400 residues,[26] with twelve residues that are fully conserved along with another seven residues that differ in only one or two of the sequences. As might be expected, the active site histidine is one of the fully conserved amino acids, but the essential tyrosine, that provides the fifth atom ligand of the heme iron, and the active site asparagine residue differ in one or two sequences, possibly because of sequencing errors. Despite the sequence similarities among all the classic heme-containing catalases there are two well defined subgroups of enzymes with polypeptide lengths of about 500 and of more than 700 residues per subunit, the small and the large subunit size catalases, respectively. Catalase HPII (hydroperoxidase II) from *Escherichia coli*, with 753 residues per subunit, is the largest heme catalase characterized.[26]

The high degree of sequence and structural similarity found among the classic heme catalases of evolutionarily distantly related organisms suggests that strong forces, not yet well understood, are restraining the differentiation of these enzymes.

PROTEIN PRODUCTION, PURIFICATION AND MOLECULAR CHARACTERIZATION

Molecular characterization protocols used in structure–function studies have created a need for the facile purification of large amounts of wild type and mutant variant protein. These have been achieved, for catalase HPII and for catalase A from *Saccharomyces cerevisiae* (SCC-A), through site-directed mutagenesis and plasmid encoded expression in catalase-deficient mutant strains.[27,28] In the case of native HPII, and of the approximately 90 mutant variants of HPII that have been obtained, cultures are grown with aeration over night at 37 °C, although some variants must be grown at 28 °C to increase the yield of protein by improving the chances of folding into a protease resistant structure. Crude extracts are fractionated with streptomycin sulfate and ammonium sulfate producing protein that is usually >75% pure. Heat treatment at 50 °C or extraction with chloroform has also been used despite the fact that they can interfere with subsequent crystallization. Ion exchange chromatography on DEAE cellulose or hydroxylapatite completes the purification.

METAL CONTENT AND COFACTORS

The prosthetic group of horse liver catalase was first identified as protoheme.[29] The heme component was extracted from purified catalase using acetone-HCl and characterized spectroscopically. In addition, the extracted heme was incorporated into hemoglobin generating a protein that was indistinguishable from native hemoglobin. Since those initial studies all small subunit size catalases have been found to contain per subunit a non-covalently bound iron protoporphyrin IX group, a *heme b* type, as the principal determinant of activity, with the usual procedure for heme quantitation involving conversion to the pyridine hemochromogens followed by spectral determination. In many of these small subunit size catalases variable percentages of the heme b cofactors appear modified towards the heme degradation pigments biliverdin or bilirubin.[30,31] In turn, in some of the large subunit catalases analyzed the corresponding heme prosthetic groups have been characterized to be an oxidized protoporphyrin IX, now known as *heme d*.[32,33] This unique type of heme, formed in the interior of the catalase molecule through a self-catalyzed reaction, has the configuration of a *cis*-hydroxychlorin γ-spirolactone, with the modifications occurring in the pyrrole ring opposite to the essential histidine.[34]

NADP(H) cofactors can also bind to some of the small subunit size catalases despite the absence of characterized nucleotide binding motifs in those enzymes.[35,36] Instead, large subunit size catalases, possessing an extra C-terminal domain with a flavodoxin-like topology, do not bind NADP(H).

ACTIVITY TEST

The two most common assays of catalase activity include the determination of oxygen evolved during catalysis using a Clark electrode[37] and the monitoring of decreased in absorbance of hydrogen peroxide at 240 nm.[38] Determination of catalase activity at normal physiological hydrogen peroxide concentrations, in the micromolar range, has also been recently developed as a chemiluminescence assay based on the reaction of luminol (5-amino-2,3-dihydro-1, 4-phthalazinedione) and NaOCl that specifically depends on the hydrogen peroxide concentration.[23]

SPECTROSCOPY

The iron atom in the resting catalases, coordinated with the four nitrogens of the porphyrin ring, is present as ferric iron (Fe(III)) in a high-spin state ($s = 5/2$).[39] The fifth iron ligand, the proximal ligand, is provided by the phenolic oxygen atom of a deprotonated tyrosine residue (Figure 1). The position of the sixth, or distal, iron ligand appears to remain empty or occupied by a weakly coordinated water molecule in resting catalases. In turn, the distal coordination position in compound I, a common intermediate in the catalytic cycles of both catalases and peroxidases, is always occupied by an oxo-oxygen atom directly coordinated with the iron (Fe(IV)) (Figure 1). Compound I in catalases, but not always in peroxidases, has a cation radical located on the heme ring itself resulting in a total of three unpaired electrons with a spin state of 3/2.[40,41]

The absorption spectra of catalases have been well documented.[10,14] The resting state enzyme exhibits a strong absorption maximum (Soret) at 407–408 nm and smaller bands at 530 nm and 630 nm. When converted to compound I, the Soret band does not shift appreciably but is decreased in intensity by about 50%. The 530 nm and 630 nm bands are red-shifted to 560 and 660, respectively. Conversion to the inactive compound II species results in a red-shift of the Soret to 430 nm along with a decrease in intensity of about 25%. The 530 nm band increases in intensity and the 630 nm band is shifted to 570 nm and increased substantially in intensity. The EPR spectrum of the native *M. lysodeikticus* enzyme exhibits transitions at $g_y = 6.58$ and $g_x = 5.56$ characteristic of high spin ferric heme. When converted to compound I by peracetic acid, the ferric heme signal at $g \sim 6$ almost completely disappears and is replaced by a strong transition at $g = 2$.[42]

X-RAY STRUCTURES OF HEME-CATALASES

Crystallization and crystallographic studies

Catalase was one of the first enzymes to be crystallized.[50] However, X-ray structural studies were considered feasible only much later, when protein crystallography had already an established methodology and new catalase crystal forms, with smaller unit cells containing a half catalase molecule in the crystal asymmetric unit, became available. The first X-ray structural determinations of catalase were made for *Penicillium vitale* catalase (PVC) at 3.5 Å resolution[51,52] and for beef liver catalase (BLC) at 2.5 Å resolution.[53,54] At present a large number of catalase crystals, suitable for high resolution structural studies, have been obtained from a diversity of biological sources using a variety of precipitants and crystallization setups, though in catalases that bind NADP(H) the partial occupancy of the cofactor can be an important source of heterogeneity[55] that might interfere with crystallization.[28] Catalase HPII from *Escherichia coli*, as a representative crystallization example, was crystallized at 22° with a protein concentration of 15 mg ml^{-1} using the hanging drop vapor diffusion method over a reservoir solution containing 15–17% PEG 3350 (Carbowax), 1.6–1.7 M LiCl (Baker) and 0.1 M Tris–HCl pH 9.0.[56] Those HPII crystals diffracted beyond 1.8 Å resolution and belong to

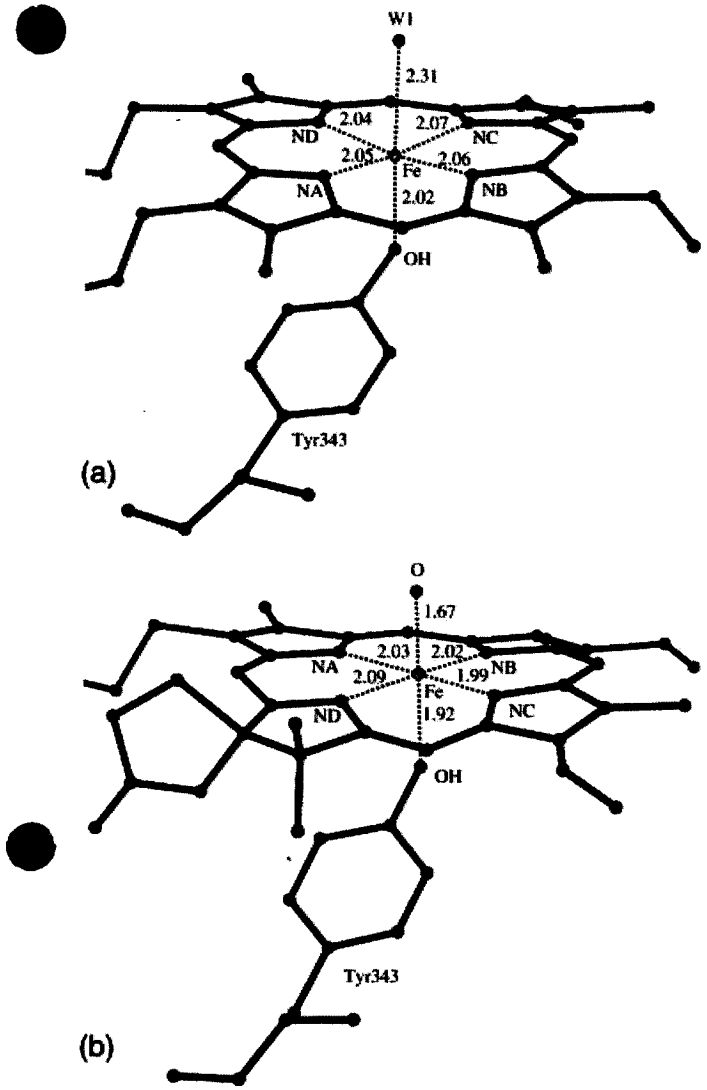

Figure 1 Views of the iron coordination: (a) in resting catalases, iron oxidation state III, as determined for native MLC at about 0.9 Å resolution; and (b) for compound I, iron oxidation state IV, as determined for PVC at 1.5 Å resolution. The macroring of the heme appears strongly buckled in both structures. The phenolic hydroxyl group of the tyrosine residue acting as the proximal ligand is, most probably, deprotonated (see text and Figure 4). The covalent modifications between heme b in MLC and heme d in PVC can be clearly identified. The water molecule in the sixth ligand position, well defined in the MLC structure, has a long coordination bond distance which suggests a weak coordination that might facilitate its removal to initiate catalysis. With respect to resting catalase the iron atom in compound I is displaced, by about 0.2 Å, towards the coordinated oxo-oxygen in the heme distal side. Drawings in this figure were made with the program BOBSCRIPT.[79]

the monoclinic space group $P2_1$, with unit cell parameters $a = 93.0$ Å, $b = 132.3$ Å, $c = 121.2$ Å and $\beta = 109.3°$, containing one molecule, a tetramer, per asymmetric unit with a solvent content of about 40%.

The refined crystal structures of seven monofunctional heme-containing catalases from different species are now available including three prokaryote enzymes, *Micrococcus lysodeikticus* catalase (MLC),[57] a peroxide-resistant mutant of *Proteus mirabilus* catalase (PMC_PR; PDB codes: 1CAE, 1CAF)[31] and HPII (PDB code: 1IPH);[27] and the eukaryote enzymes, catalase-A from *Saccharomices cerevisiae* (SCC-A; PDB code: 1A4E),[28] PVC,[58] BLC (PDB codes: 7CAT, 8CAT)[59] and catalase from human erythrocyte (HEC; PDB codes: 1DGF, 1DGB, 1DGG and 1DGH).[55]

Overall description of the structure

The structural similarity found among all heme-catalases, even higher than the expected from the sequence similarities, spans for about 460 residues per subunit. The conformation displayed by the homologous molecular regions appears to be exclusive of mono-functional heme catalases and has been referred as the 'catalase fold'.[1] The 'catalase fold' can be described, following the nomenclature used with BLC,[53] as composed of four consecutive regions along the polypeptide chain: (i) an amino terminal arm, (ii) an anti-parallel eight-stranded β-barrel domain, (iii) an extended structure that was named the 'wrapping domain' or the 'wrapping loop' and (iv) an α-helical domain.

The amino-terminal-arm region, that extends to the essential catalytic histidine, is quite variable in length ranging from 53 residues in PMC to 127 in HPII, although, from sequence analysis, most small subunit catalases appear to contain about 60 residues in their amino-terminal-arms. Helix α2 (residues 101–119 in HPII) is the first secondary structure element common to all the catalase structures available (Figure 2). The amino-terminal-arm region is involved in extensive intersubunit interactions and residues from this region contribute to define the heme pocket of a symmetry related subunit in the molecule. The extent of the intersubunit interactions increases with the length of the amino-terminal-arm region that shows a clear correlation with differences in molecular stability among catalases.[60] The catalase structures determined often show a variable number, of disordered residues at the amino end, 26 in HPII,[56] despite the restraints imposed by the intricate intermolecular interactions.

The anti-parallel eight-stranded β-barrel domain is the central feature of the catalase fold. The continuity of the hydrogen bonding within the β-barrel is interrupted between strands β4 and β5, where there are only two well defined hydrogen bonds that involve the catalytic asparagine (Figure 2). The first half of the β-barrel (β1–β4) contains most of the residues that define the heme distal side.[59,61] The second half of the β-barrel contributes to the NADP(H) binding pocket in those catalases that

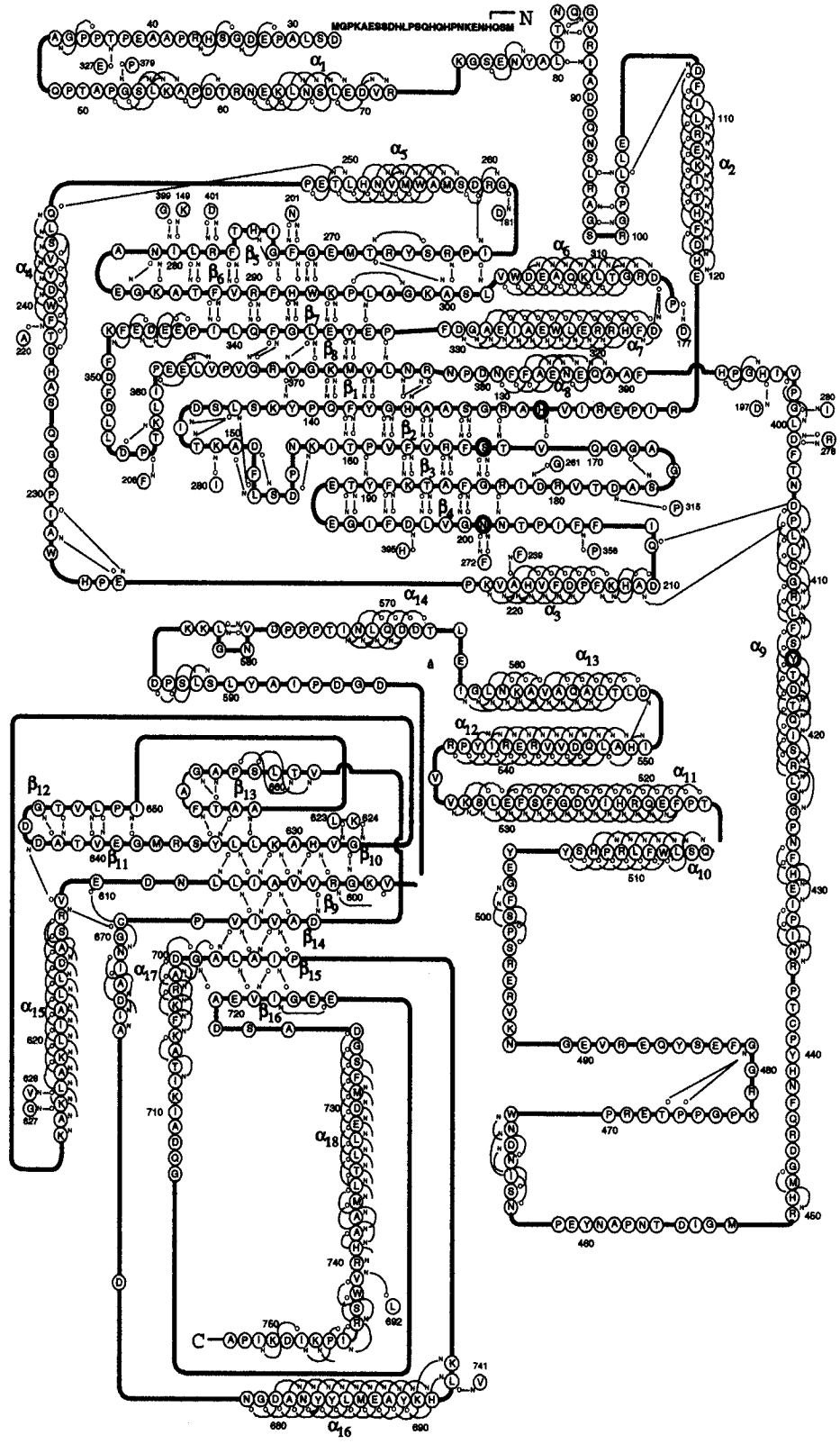

Figure 2 Main-chain hydrogen bonding network corresponding to an HPII subunit. HPII is, at present, the largest catalase molecule characterized and the nomenclature of their secondary structural elements, explicitly indicated in this figure, can be used as a common reference for all the catalase structures. The extra carboxy terminal domain, only present in the large subunit size catalases, is shown in the lower-left side of the figure. Important catalytic residues are represented with thicker circles (see text). The side chain side chain covalent bond, found only in HPII between atom N_δ from His392 and atom C_β from the essential tyrosine residue (Tyr415), has been omitted to emphasize the common features among catalases.

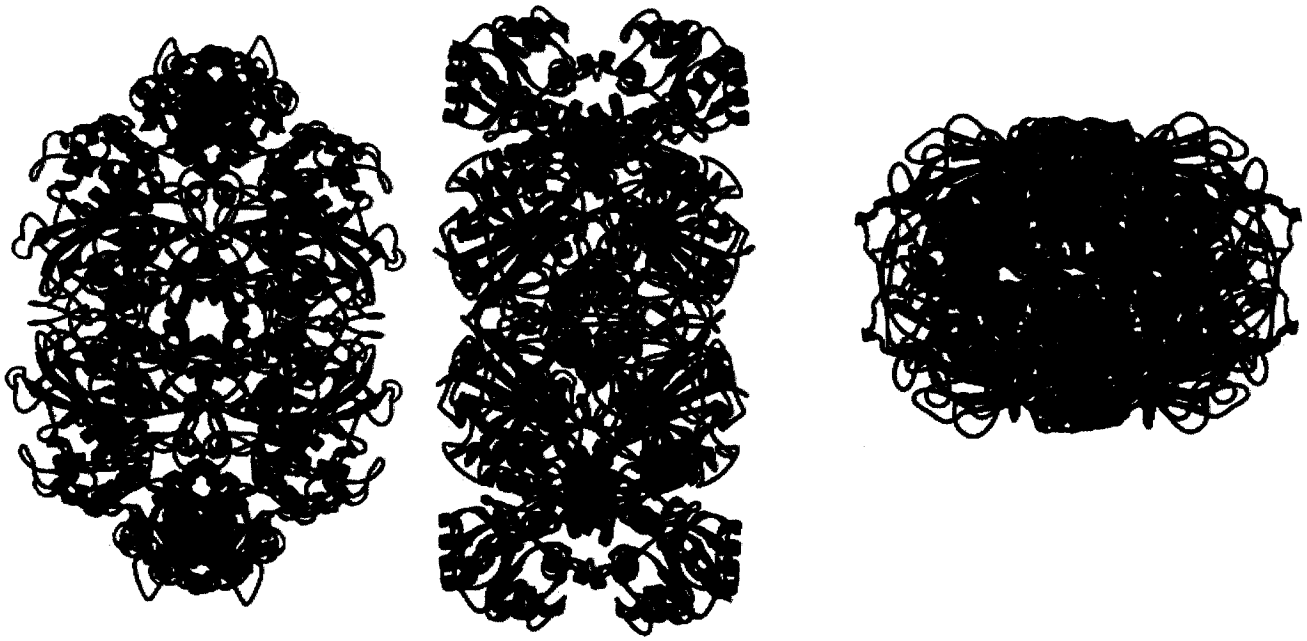

Figure 3 Views down the three molecular dyad axis (referred as P, Q and R) of the HPII tetramer. A different color is used for each subunit which allows to appreciate the extensive intsubunit interactions found in the catalase tetramers. A singular knot-like structure between Q related subunits results from the insertion of the amino-terminal arm into a narrow loop formed by residues from the wrapping domain from the neighbor subunit. This singular feature is common to all heme-containing catalases structures determined despite the diversity, both in sequence and length, of the N-terminal region. The extra carboxy terminal domain, present in the large subunit size catalases, increases only the longest molecular R axis. The figure was made with BOBSCRIPT.[79]

bind this cofactor. In all the catalase structures at least six helices are also part of the β-barrel domain, three of them (α3, α4 and α5) inserted between the two halves of the β-barrel (Figure 2).

The wrapping loop is an extended region of about 110 residues that links the globular β-barrel and α-helical domains. This region has a low content of secondary structural elements though it contains helix α9 with most of the residues that define the heme proximal side including the essential tyrosine. The wrapping loop participates in extensive intersubunit interactions particularly with residues from the amino-terminal-arm region from another subunit (see below).

The α-helical domain, with about 60–65 residues, is defined by four, continuous anti-parallel α-helices that cluster with three of the helices found between different strands of the β-barrel domain.

The structures of the two large subunit catalases determined, PVC[58] and HPII,[56] present a conspicuous extra carboxy-terminal domain of about 150 residues with a high content of secondary structure elements organized with a 'flavodoxin-like' topology (Figure 2). This extra domain, that from sequence analysis seems to be present in all the large subunit size catalases, has never been associated with nucleotide binding and other possible functional or structural roles remain unknown.

The quaternary organization of catalases also appears extremely well preserved even among very distantly related organisms. Catalase molecules are tetramers with the four subunits related to each other by three perpendicular dyad symmetries, which have often been used as the axes *P*, *Q* and *R*[54] of a molecular reference frame (Figure 3). The small subunit size catalases are roughly dumbbell-shaped with maximum dimensions of about 100 Å × 80 Å × 100 Å along the *P*, *Q* and *R* molecular axes, respectively. In the large subunit catalases only the size along the *R* axis changes significantly to a value of about 140 Å (Figure 3). A unique feature of the molecular organization of catalases is the slipping of the amino-terminal arm of one subunit through the wrapping loop of the *Q*-related subunit. This intricate intersubunit threading seems to require a deep coordination between the folding of subunits and the oligomerization process.[14,60]

Heme and heme pocket

Heme groups are deeply buried inside the catalase tetramer with iron atoms situated at about 20 Å from the nearest molecular surface. Heme pockets show extensive structural similarities among different catalases,[31,61] though, as indicated before, at least four covalent variants of the heme group have been reported: the heme b itself, the heme degradation pigments biliverdin or bilirrubin and the modified heme d group. In PVC and HPII the 'heme orientation', defined by the relative disposition of vinyl and methyl groups from pyrrole rings I and II, is mostly inverted with respect to the heme orientation found in the

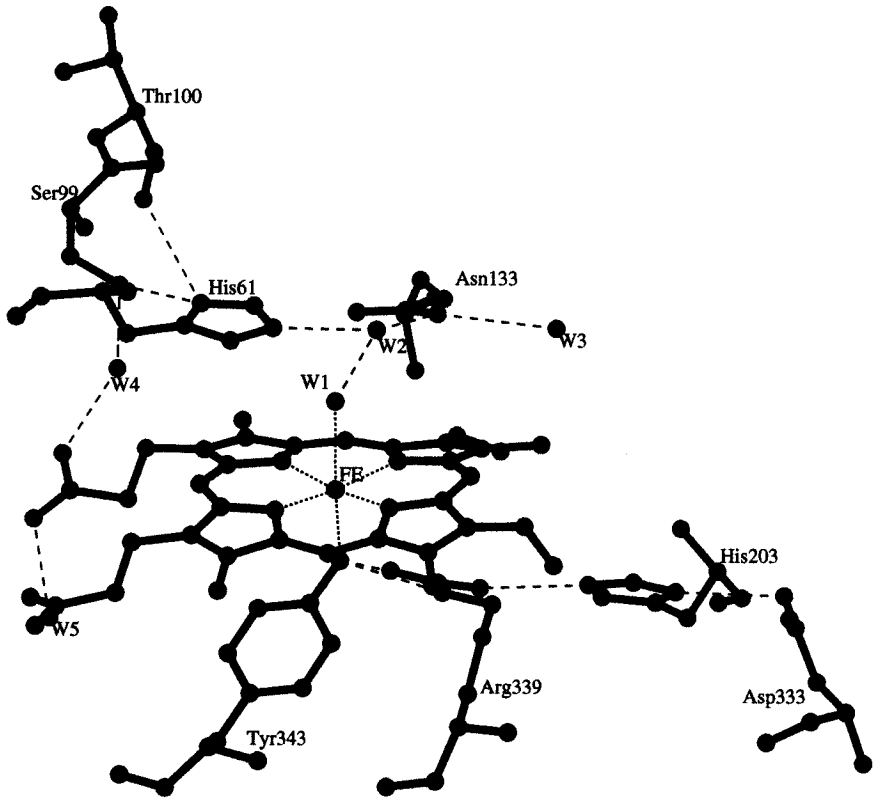

Figure 4 Heme environment in catalases as determined for native MLC (for clarity iron coordination distances, shown in Figure 1(a), are not repeated in this drawing). Only residues hydrogen bonded to the catalytically important amino acids His61 and Tyr343 are shown (see text). Conserved solvent molecules are also included, though the water closest to the heme iron (W1), well defined in MLC, appears to have only partial occupancy or large positional disorder in most catalase structures determined. The bonding geometry of the phenolic oxygen of Tyr343, particularly the presence of a double hydrogen bond with Arg339, supports the deprotonation of this tyrosine. The figure was made with BOBSCRIPT.[79]

five smaller subunit size catalase structures available[34] (Figure 4).

In catalases three residues are considered essential for catalysis: a tyrosine on the proximal side of the heme (Tyr415 in HPII) and a histidine and an asparagine on the distal side (His128 and Asn201 in HPII) (Figure 4). The oxygen of the phenolic hydroxyl group of the essential tyrosine is the proximal ligand of the heme iron, the coordination ligand L5. This oxygen, that also forms two hydrogen bonds with the N_ε and N_η atoms of a fully conserved arginine residue (Arg411 in HPII), is most likely deprotonated possessing a localized negative charge that can contribute to the stabilization of the high oxidation states of the iron in catalases.[61] On the heme distal side, the imidazole ring of the essential histidine is situated almost parallel to the heme, at a mean distance of about 3.5 Å above pyrrole ring III (pyrrole ring IV in the inverted hemes of PVC and HPII). A serine residue (Ser167 in HPII), hydrogen bonded to the N_δ atom of the essential histidine, can also have a critical role in catalysis favoring one of the tautomers of the histidine. In fact the N_δ atom of the essential histidine presents an alternative hydrogen bond with a main-chain oxygen atom (from residue Thr168 in HPII) (Figure 4), which would facilitate small rotations of the imidazole ring, as seen in the HPII variant Val169Cys (see below), that might be used during catalysis. The N_ε atom of the essential histidine is situated the closest to the heme iron, though still too far for a direct coordination, and has been assumed to mediate the transfer of hydrogen during catalysis (see below). The side-chain oxygen atom of the essential asparagine remains unbound in resting catalase, a conspicuous energetically unfavorable situation which could also have a role in catalysis, such as the stabilization of the heme radical present in compound I (see below).

The character of the heme pocket, particularly on the distal side, is strongly hydrophobic apart from the polar atoms from the functional groups, such as the essential histidine and asparagine. The hydrophobic residue preceding the essential histidine is in direct contact with the heme and appears to have a major role in selecting the shape and size of substrates that can reach the iron atom. This residue is most frequently a valine (Val127 in HPII), but it is a methionine, post-translationally oxidized to a methionine sulfone, in PMC_PR and a *cis*-proline in both MLC and SCC-A. The negatively charged propionic side chains of the

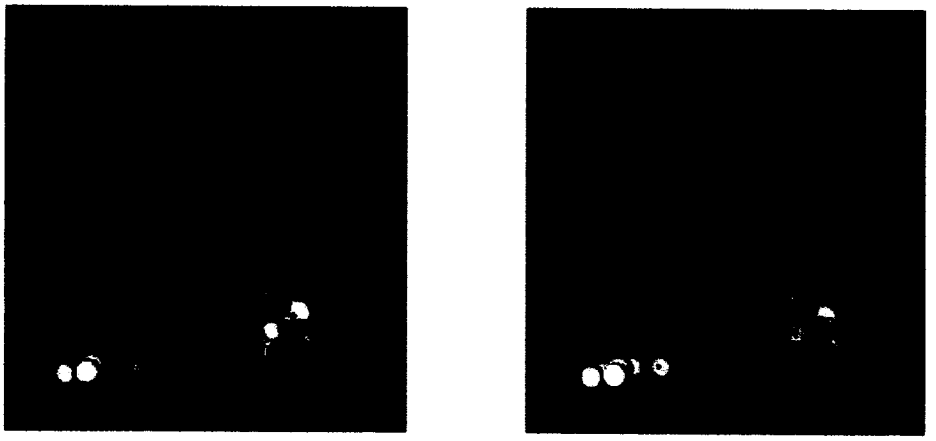

Figure 5 Detailed stereo view of the accessibility surfaces of the native SCC-A (in blue) and of the Val111Ala variant protein (yellow grid). The heme and the NADP(H) cofactors are explicitly represented as solid spheres. The solvent accessibility of the major entry channel, with a funnel shape and labeled 1 in this figure, is interrupted in the native structure only in the vicinity of residue Val111; instead this channel reaches the heme distal pocket in the structure of the Val111Ala variant (see text). In both the small and the large subunit size catalases the major channel is filled with solvent molecules except in the lower and narrower part, for about 8 Å in length before reaching the heme pocket, where no well defined solvent molecules are seen (Figure 9a). An alternative channel with two branches (labels 2 and 3 in the figure), reaching close to the heme site above and below the catalytic asparagine (Asn143 in SCC-A), has its entrance at the NADP(H) pocket. The NADP(H) cofactor when bound to one catalase subunit would seem to lock the entrance to the two branches of this alternative, lateral channel, in the corresponding subunit. At least two more paths, not shown in this figure, connecting the heme pocket and the protein exterior can be proposed.[14,31]

heme, fully buried and pointing towards the molecular center in catalases, are neutralized by a complex network of ionic and hydrogen bonding interactions primarily with residues from the wrapping domain. Residues in the wrapping domain also form most of the heme proximal pocket including the essential tyrosine coming from helix α9. Therefore, the interactions formed during the heme internalization may provide integrity to the loosely structured wrapping domain, which itself participates, as indicated before, in many subunit–subunit interactions. Residues from the β-barrel domain define the heme distal side and also the cavity lining the edges of heme pyrrole rings I, II and III in BLC, SCCA, PMC_PR or MLC (pyrrole rings II, I and IV, respectively, in the inverted heme groups).

The limited accessibility to the heme groups in catalases, deeply buried inside the molecular tetramer, requires the existence of channels for an efficient communication between the active center and the surface of the molecule. In fact, a complex network of molecular channels and cavities appears extremely well conserved, particularly among the small subunit size catalases. A major channel reaches the distal side of the heme pocket, close to the essential histidine and asparagine residues, almost perpendicularly to the plane of the heme (Figure 5). In the small subunit size catalases this channel, with a funnel shape and about 30 Å long, opens near the molecular *R* axis and becomes narrow and hydrophobic just before reaching the heme pocket. In the large subunit size catalases this channel, narrower and about 20 Å longer than in the smaller enzymes, starts following the interface between the extra carboxy terminal domain and the β-domain of an adjacent subunit. A second, bifurcated channel, approaches the heme laterally above and below the essential asparagine (Figure 5). This second, or lateral, channel emerges in the molecular surface at a location that corresponds to the NADP(H) binding pocket in catalases that bind the dinucleotide (Figure 5). In large catalases the upper branch of this lateral channel shows some discontinuities, though combined biochemical and structural analysis with the variant HPII Arg260Ala still support its role as a possible path to or from the heme.[43]

NADP(H) and NADP(H) binding pocket

NADP(H) binding to catalases was totally unexpected when it was found to occur in some mammalian catalases.[35,36] NADP(H) binding has since then been shown to be a frequent feature of small subunit size catalases from both prokaryotic and eukaryotic organisms.

The NADP(H) binding pocket, one per catalase subunit, is located towards the carboxy ends of helices α5 and α10 in a site on the molecular surface associated, as indicated above, with the entrance to the lateral channel (Figure 5).[31] Distances between the NADP(H)-binding sites of different subunits are larger than 60 Å with the nicotinamide active carbon (C^4) situated at about 20 Å from the closest heme iron atom (Figure 6).[36] Catalase residues defining the NADP(H) binding pocket are strongly conserved and the important differences in the dinucleotide binding affinities to different catalases seem to be mainly due to a single amino acid exchange: a histidine, present in enzymes with

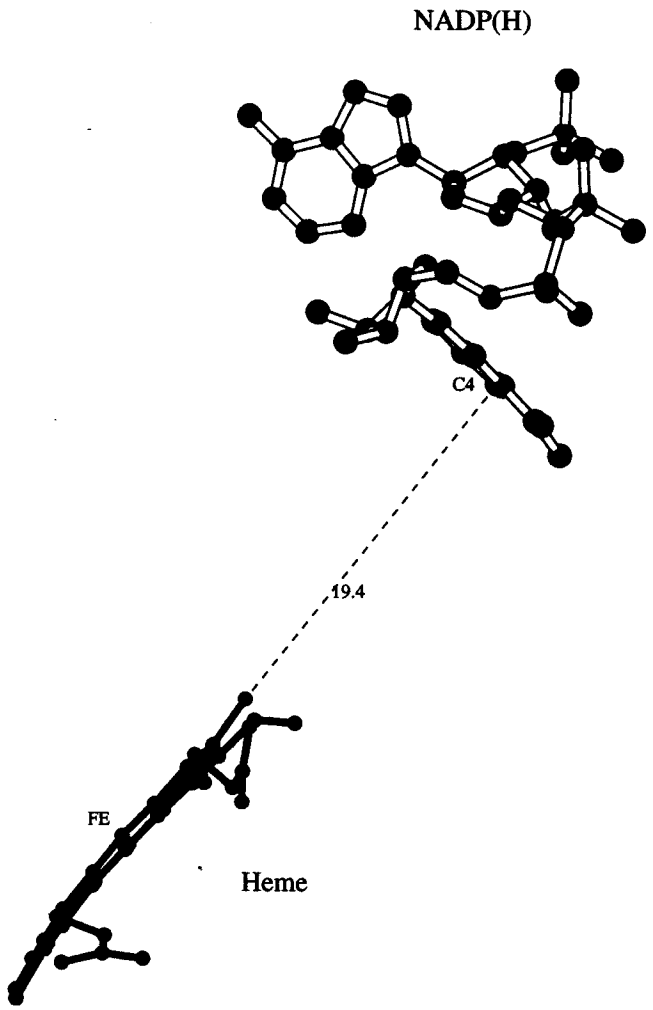

Figure 6 Relative disposition and distances between the catalytic atoms of the heme and NADP(H) cofactors found in many small subunit size catalases, as determined in the PMC_PR structure.[31] The compact conformation adopted by the bound NADP(H) is apparent. Distances between the active center atoms of the two cofactors suggest the existence of molecular electronic pathways in catalases. The figure was made with program BOBSCRIPT.[79]

high NADPH binding affinity (His304 in BLC), for a glutamine in the low affinity catalases (Gln302 in SCC-A).[28] A comparative analysis of the PMC_PR and HEC structures with and without NADPH showed that no important rearrangements are induced by the dinucleotide binding to catalases.[31,55] Bound NADP(H) molecules in PMC_PR, BLC and HEC have right-handed helical conformations, with the two bases within 4 Å of each other (Figure 6). NADP(H) when bound to proteins is generally found in an extended conformation and only the NADP(H) in flavin reductase P exists in a more compact structure than in catalases.[62] In the SCC-A and MLC structures, the nicotinamide portion of NADP(H) shows larger disorders than the adenine portion suggesting that NADP(H) binding is driven by adenine while the nicotinamide interactions, sensitive to the oxidation state of the dinucleotide, might have a variable contribution.[28] The pocket corresponding to the NADP(H) binding site in small subunit catalases appears partially filled in the large subunit enzymes, such as HPII and PVC, by residues from the protein segment that joins the α-helical and the flavodoxin terminal domains. An entrance to the lateral channel is kept in the large subunit size catalases in exactly the same location as in the smaller catalases, despite the absence of NADP(H) binding to the large enzymes.

The biochemical function of NADP(H) in catalases is not yet fully understood. It seems clear that one likely role is protection of the enzyme against inactivation by its own substrate, mainly in conditions of low-peroxide concentrations.[63] It has also been shown that NADP(H) is essential for the dismutation of small peroxides, other than hydrogen peroxide, although the contribution of the cofactor to this reaction is unclear.[64] Hypotheses explaining the interactions of NADP(H) with the heme intermediates, particularly compound II (see below), and the electron transfer paths between the heme and the nucleotide have been intensively investigated[65–68] and recently reviewed.[14]

FUNCTIONAL ASPECTS

Oxidation–reduction potentials

The redox potentials of the reaction intermediates of catalase have not been reported.

Kinetics

The catalatic reaction of catalases has been extensively analyzed by a variety of spectroscopic techniques, and the kinetic implications of these studies have also been recently reviewed.[14] One very significant caution reiterated in that review is that most reports of Michaelis–Menten kinetic constants attributed to catalases can be misleading because the enzyme can neither be saturated with substrate hydrogen peroxide before it is inactivated nor has a true enzyme–substrate complex been directly observed before compound I in catalases, in other words, catalases do not follow typical Michaelis–Menten kinetics. The consequence is that all reports of the constants, K_m and k_{cat}, are really 'apparent' constants and must be interpreted in this light.

It is not possible to define a single value to any of the kinetic constants that would be applicable to all catalases. There is extensive variation in these constants among heme-catalases from different sources often arising, at least in part, from subtle sequence and structural variations among the different enzymes which influence substrate accessibility and product exhaust. For example, enzyme

activities can vary over a 10-fold range from 14 000 units per mg for *E. coli* HPII and 30 000 units per mg for bovine catalase to 180 000 units per mg for the catalase from *Serratia marsescens*. These values were all determined in an oxygraph using 60 mM H_2O_2, but significant variations are caused by only small changes in substrate concentration making a comparison of literature values very difficult. The picture is further complicated by varying sensitivities to inactivation of catalase by its own substrate, H_2O_2. For example, BLC is inactivated at H_2O_2 concentrations above 0.3 M whereas *E. coli* HPII loses activity only above 3 M H_2O_2[43] and this in turn affects the observed K_m values. The kinetic constants are also dependent on the assay method employed, whether by extrapolation of absorbance changes at low H_2O_2 concentrations or direct assay of oxygen evolution in an oxygraph at higher H_2O_2 concentrations. With these caveats in mind, the following values were determined for BLC and HPII using the oxygraph assay method:[43] for BLC, $K_m = 70\,mM$ and $k_{cat} = 3.7 \times 10^5$ (at 300 mM H_2O_2), and for HPII, $K_m = 450\,mM$ and $k_{cat} = 1.4 \times 10^5$ (at 3 M H_2O_2). However, K_m and k_{cat} values of 1.1 M and 3.8×10^7, respectively, have also been reported for heme-catalases.[44]

Reaction pathway

The catalatic dismutation of hydrogen peroxide by heme catalases takes place in two discrete stages, each employing one hydrogen peroxide molecule.[11,45,46] The first substrate molecule is reduced to water, oxidizing catalase to an oxyferryl specie, compound I, in which one oxidation equivalent is on the iron and a second oxidation equivalent is delocalized as the porphyrin cation radical (Equation (2)).[47,48]

$$\text{Enzyme (Por–Fe(III))} + H_2O_2 \rightarrow \text{Compound I (Por}^{+}\text{–Fe(IV)} = O) + H_2O \quad (2)$$

A second hydrogen peroxide molecule can then complete the catalatic cycle reducing compound I back to the native Fe(III) state along with the generation of water and molecular oxygen (Equation (3)).

$$\text{Compound I (Por}^{+}\text{–Fe(IV)} = O) + H_2O_2 \rightarrow \text{Enzyme (Por–Fe(III))} + H_2O + O_2 \quad (3)$$

Alternatively, the resting catalase can be recovered from compound I by two-electron oxidation peroxidatic reactions of some small organic substrates such as aliphatic alcohols. In most small subunit catalases, compound I can also be reduced *via* one electron reduction of the porphyrin radical resulting in the formation of an alternative ferryl intermediate called compound II (Equation (4)). Electrons could be derived either from exogenous donors, as in most peroxidases, or from endogenous donors not yet well identified in catalases.

$$\text{Compound I (Por}^{+}\text{–Fe(IV)} = O) + AH \rightarrow \text{Compound II (Por–Fe(IV)} = O) + H^{+} + A^{\cdot} \quad (4)$$

Compound II can either be converted back to the native enzyme by a second one electron reduction reaction or it can react with another molecule of peroxide to give compound III (formally Fe(VI)), a catalytically inactive intermediate. However, the rates of one electron reaction are slow in catalases and compound II has never been identified in the large subunit enzymes which do not bind NADPH. This observation seems to support the hypothesis that the dinucleotide cofactor has a role in preventing the accumulation of compound II in small subunit enzymes as indicated above.[49]

A detailed account of the diverse catalytic possibilities of heme-catalases has been recently reviewed.[14]

FUNCTIONAL DERIVATIVES

X-ray structures of compounds I and II

The crystal structures of catalase intermediate compounds I and II were first trapped with PMC_PR using X-ray fast data-collection techniques.[69] The analysis of the structures of the two compounds, at 2.7 Å resolution, revealed only minor local rearrangements relative to the native enzyme. In both compounds the iron appears slightly displaced above the heme ring towards the bound oxygen, clearly visible in the position of the distal side iron ligand. In compound I, but not in compound II, the presence of an extra peak in the electron density map, situated in the heme proximal side at about 18 Å from the iron, was interpreted as a transiently bound anion.

The structures of compound I in PVC (Figures 1 and 7) and of (most likely) compound II in MLC have also been recently studied, at 1.8 and 1.6 Å resolution respectively, using standard X-ray data-collection methods. These structures, prepared in both cases by soaking crystals of the native catalases with peracetic acid and afterwards flash cooling them to liquid nitrogen temperatures, confirm the absence of major structural rearrangements with respect to the resting enzymes and also the displacement of the iron atom towards the bound ligand on the heme distal side in both compounds. However, no extra density, similar to that reported for compound I in PMC_PR, has been identified in the structure of compound I in PVC. Instead, the structure of PVC compound I contains at least one acetate molecule, derived either from the peracetic acid or from the acetate buffer, located in the main channel at about 15 Å above the heme (Figure 7). In

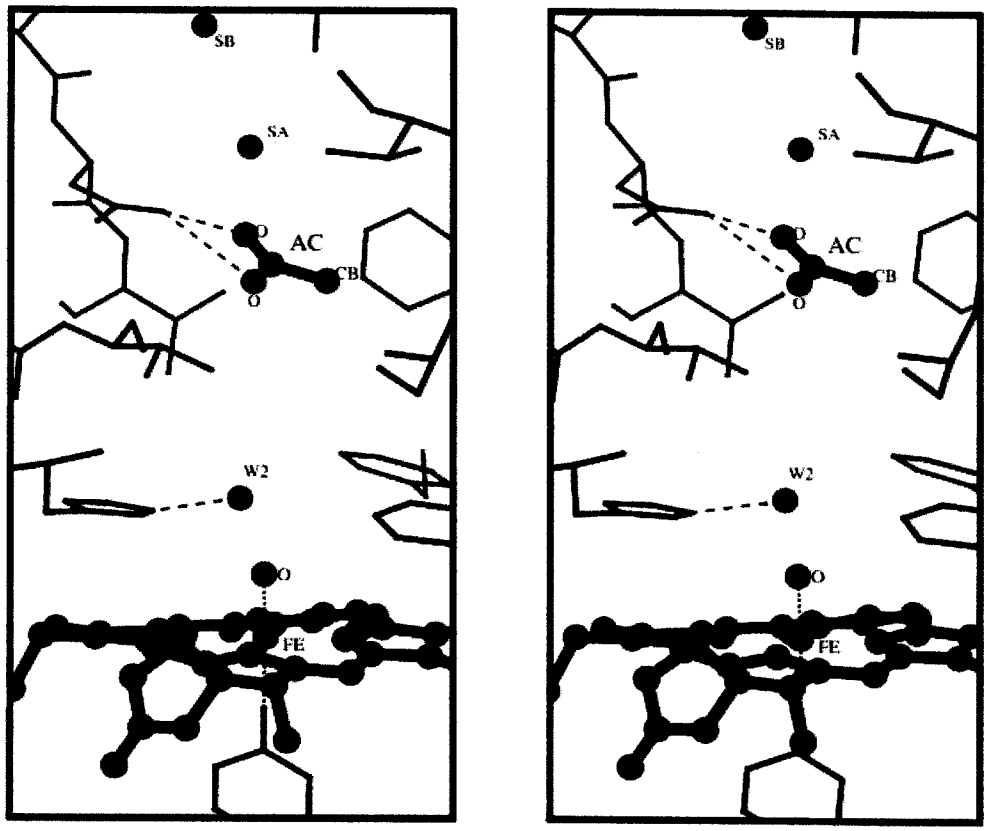

Figure 7 Stereo view of the heme distal side pocket and of the lower part of the major heme channel in the PVC compound I structure (iron coordination distances are given in Figure 1(b)). One solvent molecule, corresponding to the position of solvent molecule W2 in Figure 4 and also named W2 in here, is well defined in the heme distal side besides the oxo-oxygen coordinated with the heme iron. Solvent molecules are absent in the lower part of the major channel reaching the heme though, at about 8 Å from W2, an acetate molecule, hydrogen bonded to a putative aspartic residue, and farther up two more solvent molecules, labelled SA and SB, have been identified (compare with Figure 9(a) and (b)). The figure was made with BOBSCRIPT.[79]

both the PMC_PR and the PVC compound I structures the coordinated oxygen is situated at 1.7–1.8 Å above the iron atom, but at distances larger than 3.3 Å both from the N_ε atom of the essential histidine and from the single solvent molecule found inside the distal heme pocket. This solvent molecule is hydrogen bonded to the N_ε and N_δ atoms of the essential histidine and asparagine residues, respectively (Figure 7). In the structure of compound I, as also in resting native catalases, no well defined solvent molecules are found in the lower part of the main channel (Figure 7).[28]

Amino triazole and azide complexes

The structure, at 1.8 Å resolution, of PVC complexed with the specific catalase inhibitor 3-amino-1,2,4-triazole (AT) shows a hydrogen bond between the N^1 AT atom and the side chain oxygen atom of the essential asparagine and also, as anticipated,[70] a covalent bond of the C^5 atom from the AT molecule with the N_ε atom of the essential histidine (Figure 8). All the AT atoms are situated about 3.5 Å above the heme macro-ring eliminating the possibility of the proposed existence of a direct coordination between the AT molecule and the iron atom. The coplanarity of the imidazole and AT rings could be reflecting a partial resonance between the two aromatic rings but also the restraints imposed by the distal heme pocket geometry, particularly by the planarity of the heme group itself. In fact, in the PVC–AT complex structure no space is left for solvent molecules and even some displacement of the conserved Phe141 (PVC sequence, derived from the X-ray structure, which corresponds to Phe206 in HPII) is required (Figure 8). Therefore, catalases with reduced distal side pockets, like PMC_PR, can be expected to have a diminished sensibility towards inhibition by AT.[31] The structure of the PVC–AT complex offers structural indications, such as the proper geometry to bind simultaneously to the histidine and asparagine, of the specificity of AT for catalases particularly with respect both to catalase-peroxidases and to peroxidases.

The crystal structure of catalase complexed with the classical heme inhibitor azide have been obtained for both SCCA and HPII.[28,71] In both structures there is a direct coordination between the heme iron and the azide nitrogen atom N^1, with a coordination angle ($Fe–N^1–N^2$) of about

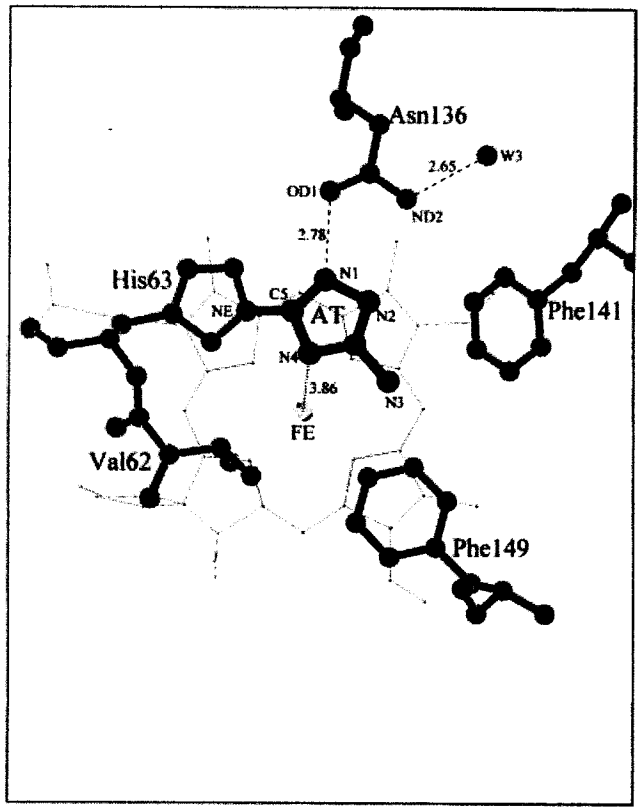

Figure 8 View down the heme distal side of the catalase inhibitor 3-amino-1,2,4-triazole (AT) complexed with PVC.[63] The AT molecule, stacked above the heme, is covalently bound to the essential histidine and hydrogen bonds the catalytic asparagine. However, with the shortest distance at 3.86 Å no direct coordination can be established between the iron in the heme and the AT molecule. The figure was made with BOBSCRIPT.[79]

130 ° as expected for the hybridization in the azide molecule. Azide atoms N^2 and N^3 are both situated at distances of only about 3.0 Å from the N_ε atom of the essential histidine. No solvent molecules are seen in contact with the azide molecule, which appears to be replacing the solvent found in the heme distal pocket of resting catalases. The geometry of the azide complex, in particular the direct coordination of the azide molecule with the iron atom, confirms that the inhibition mechanism of azide is similar in catalases to the one reported for other heme enzymes.

X-ray structures of mutant catalases

Combined structural and site directed mutagenesis studies have been extensively done in HPII and, to a lesser extent, in SCC-A. In HPII these combined analyses have included modifications affecting: (i) the accessibility to the heme, both throughout the major and the lateral channels,[28] (ii) the catalytic essential residues,[72] (iii) the covalent structure of the molecule, including alterations in the heme oxidation or extra bonds between residues,[73] and (iv) the folding and oligomerization processes.[60] Combined studies in SCC-A have concentrated on the analysis of mutations in the lower part of the main channel, particularly residue Val111, which when replaced by an alanine presents some reduction in catalatic activity but important increments of peroxidatic activity for substrates bulkier than ethanol.[74]

HPII variants Val169Cys, His392Gln and His392Glu resulted in modifications of the covalent structure of the enzyme that affected directly to either the His128 or the Tyr415 essential residues.[73] The HPII variant Val169Cys, intended to allow selective changes of the major channel diameter at the entrance of the distal pocket, contains a new type of covalent bond formed between a carbon atom from the imidazole ring of the essential histidine (His128) and the sulfur atom of the modified residue (Cys169) (Figure 9). This variant enzyme has only a residual catalytic activity and presents an unmodified heme b group instead of the heme d found in HPII, supporting the relationship between catalase activity and modifications on the heme. The Val169Cys structure also shows, in the final part of the major channel, a continuous chain of well defined water molecules whose disposition and interactions were assumed to reflect the organization of hydrogen peroxide substrate molecules entering towards the heme pocket in active catalase (Figure 9).

The self-catalyzed oxidation of heme b to heme d has been linked with the formation of the covalent bond between the N_δ atom of His392 and the C_β atom of the essential tyrosine (Tyr415), a singular post-transcriptional modification found in native HPII.[71] PVC, like HPII, contains heme d but, unlike HPII, contains an unmodified essential tyrosine, a result of having a glutamine at the position corresponding to His392 in HPII. The His392Gln variant of HPII retains 75% of native catalytic activity and contains heme b, in turn the His392Glu variant exhibits only 25% of native activity and contains a mixture of heme b and *cis* and *trans* isomers of heme d. These results seem to indicate that heme d is not strictly required for activity in the large subunit size catalases, therefore questioning the meaning of this self-catalyzed heme modification.

The catalytic roles of the essential histidine and asparagine residues have been investigated by analyzing the two inactive, His128Asn and His128Ala, and the two weakly active, Asn201Ala and Asn201His, HPII variants. The structures of the four variant proteins show a solvent organization strongly altered with respect to native HPII in the vicinity of the heme pocket. The main channel in the His128Asn and His128Ala structures is filled with a continuous chain of hydrogen bonded water molecules spanning from the molecular surface to the heme distal pockets. In these two essential histidine HPII variants the disposition and interactions of the chained water molecules, particularly in the lower part of the channel, might well be reflecting the organization of hydrogen peroxide substrates when entering the native

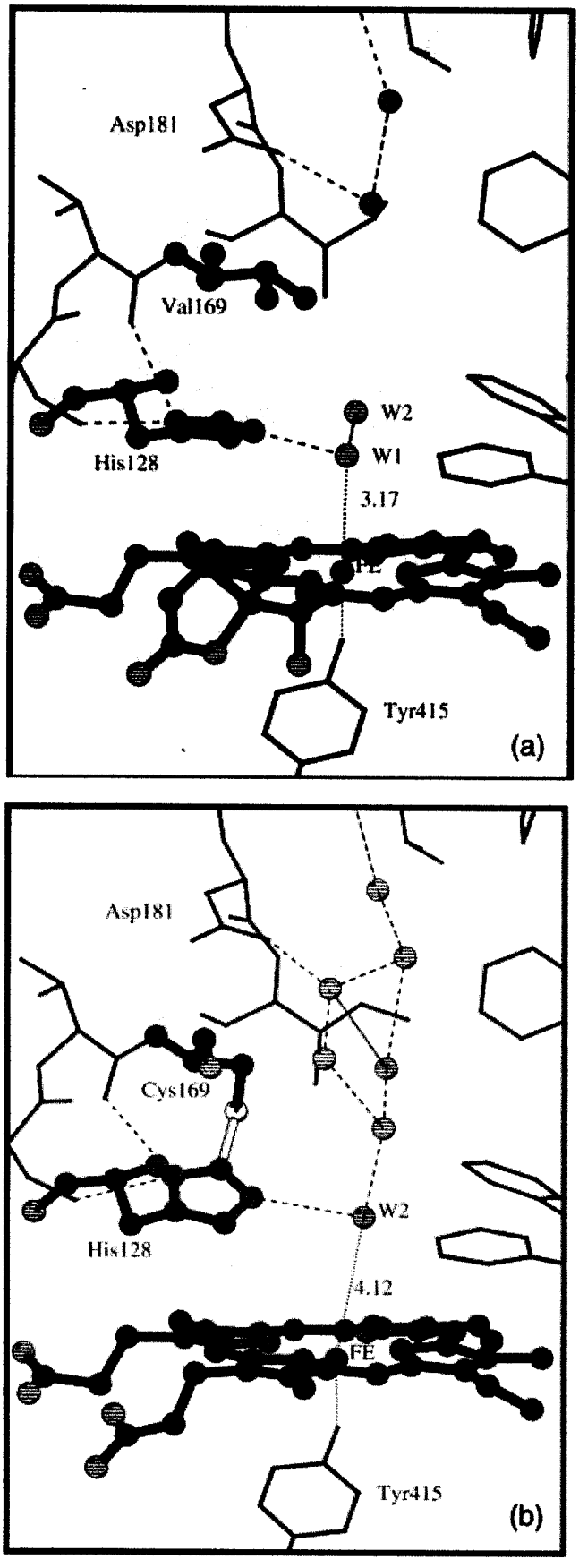

enzyme, as also indicated above for the HPII variant Val169Cys.[73]

CATALYTIC MECHANISMS

Compound I formation and reduction: peroxidatic reaction

Structure-based hypothetical catalytic mechanisms for compound I formation and reduction were formulated when the native structures of BLC and PVC became available[61] taking into account the approach followed with cytochrome C peroxidase (CCP).[75] Particularly relevant new information concerning the catalytic mechanism in catalases can now be included from: (i) the catalytic and structural peculiarities of a number of catalase variants,[34,71–73] (ii) the compound I and compound II structures referred above,[69] (iii) the accurate determination of the solvent organization in the vicinity of the heme group,[56,73] (iv) the detailed structural information of some of the catalase structures determined, particularly MLC refined at 0.9 Å resolution and (v) the deeper understanding of heme enzymes, in particular, of heme peroxidases.[76]

Although the new experimental data now available is consistent with the catalytic mechanism that had been proposed for catalases,[61] some considerations extending those ideas should be added. In the proposed catalytic mechanism ethyl-hydrogen peroxide was used as the model substrate of the overall peroxidatic reaction:

$$CH_3CH_2OOH \rightarrow \{CH_3CH_2OH + H_2O\}$$

$$\rightarrow CH_3CHO + H_2O$$

In a formal sense the compound I formation process, with an oxygen bound to a ferryl iron with a porphyrin-centered π radical, requires the transfer of the hydrogen atom from O(2) to O(1) (oxygens from the hydroperoxide are designated as R–O(1)–O(2)–H and the chirotopic methylene hydrogens as H_R and H_S). After the transfer, the substrate becomes an acyl alcohol which can itself act as a substrate for the newly formed compound I reducing it back to the native enzyme. This second reaction step, equivalent to adding ethanol as an external substrate when compound I is already present, produces water and an aldehyde (Figure 10).

Figure 9 Views of the heme distal side pocket and of the lower part of the major channel in wild type HPII (a) and in the Val169Cys variant (b). In the Val169Cys variant structure a chain of well defined solvent molecules, not visible in the structure of the wild type enzyme, fills the major channel reaching the distal pocket. In the variant protein a covalent bond is formed between the sulfur atom of the replaced residue (Cys169) and the carbon atom C_ε from the imidazole ring of the essential histidine (His128). The figure was made with BOBSCRIPT.[79]

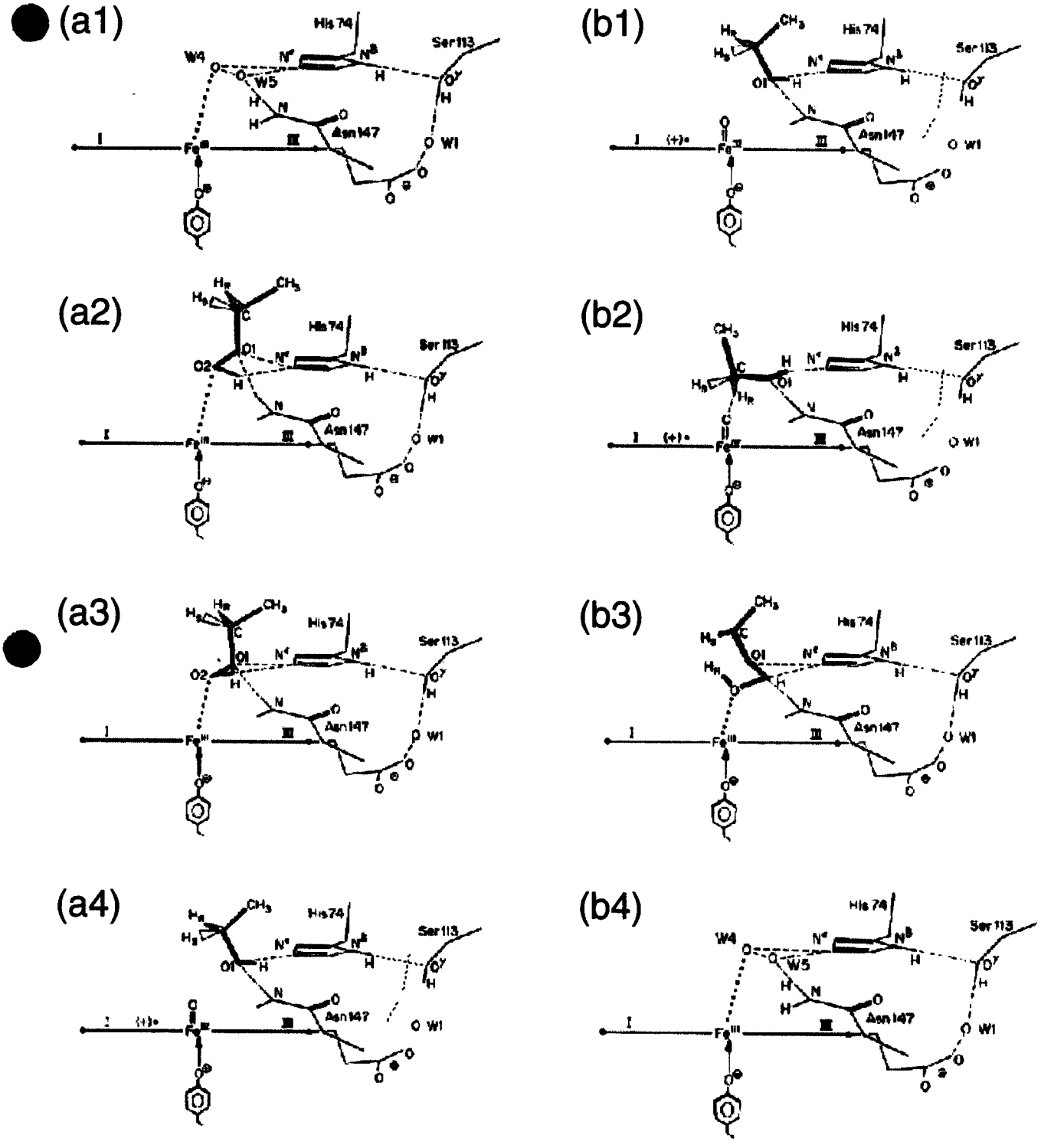

Figure 10 Schematic representations of successive hypothetical steps in the formation of compound I (a) and of the reduction of compound I back to the resting enzyme (b). (a1) Resting catalase with the two solvent molecules found in the MLC structure (Figure 4). (a2) Ethyl-hydrogen peroxide has been used as the model substrate, with the three hydrogen substrate atoms involved in catalysis explicitly represented. (a3) Transfer of the hydrogen atom between the oxygens of the peroxide (H is bound transiently to both O(1) and O(2)). (a4) Compound I structure with the newly formed alcohol molecule (ethanol) still in the distal pocket. (b1) Complex between the substrate (ethanol) and Compound I. Although in a peroxidatic reaction this step can be completely independent from that in (a4), the same figure is used to emphasize the possibility of having a continuous reaction as observed for certain substrates. (b2) Abstraction of the H_R hydrogen by the oxo-oxygen. (b3) Transfer of the alcohol hydrogen towards the oxo-oxygen (or hydroxyl ion) with aldehyde formation. (b4) Reaction completion returning to the resting enzyme configuration.

It appears that the essential features of the O–O bond heterolysis leading to formation of compound I can be similar in heme catalases and in heme peroxidases.[75] In both systems the main catalytic residue is a histidine which presents a favored imidazole tautomer with a proton on the N_δ atom while N_ε, oriented closer to the Fe atom, participates directly in the catalytic transfer of hydrogen. Furthermore, the substrate peroxide interacts simultaneously with two residues on the distal side of the heme, the essential histidine and an asparagine in catalases, or the catalytic histidine and an arginine in heme peroxidases. However, one significant difference between catalases and peroxidases lies in the identity of the proximal iron ligand: while a histidine is often found in heme peroxidases, a deprotonated tyrosine is invariably present in catalases. The tyrosinate ligand, reinforced by a charge-relay system likely acting in the heme proximal side,[55] suggests a catalytic mechanism dominated by a strong electronic push from the Fe–tyrosine pair that would compensate the weak electronic pull that can be expected to be provided by the catalytic asparagine. In peroxidases the Fe-histidine pair, with the histidine as the proximal ligand, would only give a weak electronic push even if reinforced by an interaction of the histidine with a neighbor aspartic residue (Asp235 in CCP). This weaker push would be compensated by the stronger electronic pull from the positively charged catalytic arginine found in many peroxidases (Arg48 in CCP). Other differences between the active center organizations in peroxidases and catalases were assumed to have also a role in facilitating concerted transformations in catalases leading to compound I formation. In particular the different orientation of the essential histidine with respect to the heme could allow the existence of a second charge-relay system, situated in the heme distal side between the histidine and one of the heme propionic groups.[61] However, differences between active centers in catalases and peroxidases are expected to be mainly reflecting different catalytic requirements for compound I reduction in the two types of enzymes.

Peroxidases prefer one-electron donors reducing compound I in two distinct reaction steps *via* compound II, whereas catalases prefer two-electron donors. Several explanations can be proposed to rationalize the characteristic low reactivity of catalases in one-electron peroxidations: (i) steric constraints could play a major role in the decreased turnover of substrates like phenols and aromatic amines by catalases. Accordingly, the large subunit catalases with a longer and narrower entrance channel would be expected to show, as experimentally observed, a lower tendency to give compound II.[2] (ii) The destabilization of compound II in catalases. (iii) The stabilization on the heme ring of the radical cation, which provides the first electron transferred in most one-electron reduction steps. This increased stability may, in turn, be contributed by: (a) the strong hydrophobic character of the heme environment in catalases, with the direct stacking of two phenylalanine side chains on the heme,[28,31,61] (b) the existence of unbound polar atoms close to the heme ring such as the side chain oxygen of the essential asparagine,[28] (c) the organization of the charge-relay system likely acting on the heme proximal side[55] or (d) the altered resonance structure of the heme due to either the strong bending of the macro ring observed in all the catalase structures analyzed,[31,61] or to the oxidation of one of the heme pyrrole groups as found in heme d,[34] or to the interactions with the neighbor aromatic residues, including stacking with the essential histidine.

Hydrogen peroxide as substrate: catalatic reaction

Because steps followed by the catalatic reaction in catalases were assumed to be similar to the peroxidatic mechanisms, the larger number of binding modes for hydrogen peroxide was proposed to be the main reason for the higher efficiency of the catalatic reaction in catalases.[61] However, the recent data about the solvent organization, in the vicinity of the heme, and about the catalytic activities of a number of catalase variants, suggests that molecular channels can also have a major contribution to the catalatic efficiency by selecting and pre-orienting the hydrogen peroxide substrate specifically. Lining up several molecules of hydrogen peroxide inside the channels, before reaching the heme pocket, would overcome the restricted accessibility of the heme active center in catalases explaining, at least in part, the fast turnover rate of the catalatic reaction. This hypothetical 'chain reaction' mechanism would be consistent with the high apparent K_M values of catalases for hydrogen peroxide, a reflection of an inefficient reaction at low concentrations when the chain of substrates would not be easily maintained.[46] The high selectivity towards hydrogen peroxide has been proposed to rely on an accurate 'molecular ruler' mechanism,[55] though solvent variations in a number of HPII variants seem to require alternative explanations,[72] pending the direct observation of hydrogen peroxide inside catalase.

The steady flow of substrates and products required to achieve the observed reaction rates in catalases[77] appears unfeasible if both have to move in and out simultaneously through the narrow neck of the major catalase channel,[28] even more so if incoming substrates are chained to each other. Alternative paths seem necessary to maintain a continuous flow, reaching to and from the heme, without mutual obstruction. These alternative ways are expected to appear obstructed in the resting catalases, to avoid the entrance of undesired substrates or inhibitors in the heme active center,[60] opening only during catalysis according to the 'back door' mechanism principle.[78] The lateral bifurcated channel, whose entrance is associated with the NADP(H) binding pocket, is a clear candidate for such an

alternative path to the heme, but other possibilities have also been considered.[28,31]

Therefore, for hydrogen peroxide the specific catalatic reaction achieved by heme-catalases might proceed as a cooperative, 'chain-like', substrate inlet to the heme active center concerted with a 'back-door' mechanism for the exit of products.

CONCLUSIONS

Heme-catalases are ubiquitous redox enzymes that protect against the deleterious effects of small peroxides, though the whole range of biological roles played by these enzymes appears to be much larger. A number of basic questions related with the molecular functioning and the biochemistry of heme-catalases remain open, despite the wealth of biological, biochemical and structural information now available. Part of the difficulties in reaching a deeper understanding seem due to the singularity of the catalytic mechanisms in heme-catalases that, though centered around the heme iron atom, require the critical contribution of long and intricate molecular channels.

The intensive and prolonged research around heme-catalases can still continue occupying biochemists for many more years.

REFERENCES

1 J Bravo, I Fita, P Gouet, HM Jouve, W Melik-Adamyan and GN Murshudov, in JG Scandalios (ed.), *Oxidative stress and the molecular biology of antioxidant defenses*, Cold Spring Harbor Laboratory Press, Raleigh, pp 407–45 (1997).

2 M Zamocky and F Koller, *Progress in Biophysics and Molecular Biology*, **72**, 19–66 (1999).

3 WF Beyer and I Fridovich, *Biochemistry*, **21**, 6460–7 (1985).

4 VV Barynin, AA Vagin, VR Melik-Adamyan, AI Grebenko, SV Khangulov, AN Popov, ME Andrianova and BK Vainshtein, *Sov Phys Crystallogr*, **31**, 457–9 (1986).

5 DW Christianson, *Prog Biophys Molec Biol*, **67**, 217–52 (1997).

6 MW Fraaije, HP Roubroeks, WR Hagen and WJH Van Berkel, *Eur J Biochem*, **235**, 192–8 (1996).

7 H Ruis and F Koller, in JG Scandalios (ed.), *Oxidative stress and the molecular biology of antioxidant defenses*, Cold Spring Harbor Laboratory Press, Raleigh, pp 309–42 (1997).

8 JG Scandalios, L Guan and AN Polidoros, in JG Scandalios (ed.), *Oxidative stress and the molecular biology of antioxidant defenses*, Cold Spring Harbor Laboratory Press, Raleigh, pp 343–406 (1997).

9 O Loew, *US Dept of Agric Repts*, **65**, 5 (1900).

10 A Deisseroth and AL Dounce, *Physiological Reviews*, **50**, 319–74 (1970).

11 GR Schonbaum and B Chance, in PD Boyer (ed.), *The Enzymes*, Vol 13, Academic Press, New York, pp 363–408 (1976).

12 C Masters and D Crane, *The peroxisome: a vital organelle*, Cambridge University Press, Cambridge (1995).

13 PC Loewen, in JG Scandalios (ed.), *Oxidative stress and the molecular biology of antioxidant defenses*, Cold Spring Harbor Laboratory Press, Raleigh, pp 273–308 (1997).

14 P Nicholls, I Fita and PC Loewen, Advances in Inorganic Chemistry, Vol. 51 in AG Sykes (ed.) and G Mauk (co-ed.), Academic Press, pp 51–106 (2001).

15 CJ Masters and RS Holmes, *Physiol Rev*, **57**, 816–82 (1977).

16 JG Scandalios, WF Tong and DG Roupakias, *Mol Gen Genet*, **179**, 33–41 (1980).

17 JG Scandalios, *Proc Natl Acad Sci*, **53**, 1035–40 (1965).

18 RS Holmes and CJ Masters, *Arch Biochem Biophys*, **148**, 217–33 (1972).

19 M Pegg, DI Crane and CJ Masters, *Biochem Intl*, **122**, 831–8 (1986).

20 RS Holmes and CJ Masters, *Biochim Biophys Acta*, **191**, 488–90 (1969).

21 CJ Masters and RS Holmes, *TIBS*, 233–6 (1979).

22 N Oshino, R Oshino and B Chance, *Biochem J*, **131**, 555–67 (1973).

23 S Mueller, HD Riedel and W Stremmel, *Anal Biochem*, **245**, 55–60 (1997).

24 AU Khan and T Wilson, *Chem Biol*, **2**, 437–45 (1995).

25 RH Burdon, *Free Radicals Biol Med*, 775–94 (1995).

26 MG Klotz, GR Klassen and PC Loewen, *Mol Biol Evol*, **14**, 951–8 (1997).

27 J Bravo, N Verdaguer, J Tormo, C Betzel, J Switala, PC Loewen and I Fita, *Structure*, **3**, 491–502 (1995).

28 MJ Maté, M Zamocky, LM Nykyri, C Herzog, PM Alzari, C Betzel, F Koller and I Fita, *J Mol Biol*, **286**, 135–49 (1999).

29 KG Stern, *J Biol Chem*, **112**, 661–9 (1936).

30 RB Frydman, ML Tomaro, J Awruch and B Frydman, *Biochem Biophys Res Commun*, **121**, 249–54 (1984).

31 P Gouet, HM Jouve and O Dideberg, *J Mol Biol*, **249**, 933–54 (1995).

32 JT Chiu, PC Loewen, J Switala, RB Gennis and R Timkovich, *J Am Chem Soc*, **111**, 7046–50 (1989).

33 R Timkovich and LL Bondoc, *Adv Biophys Chem*, **1**, 203–47 (1990).

34 GN Murshudov, AI Grebenko, VV Barynin, Z Dauter, KS Wilson, BK Vainshtein, WR Melik-Adamyan, J Bravo, JM Ferrán, JC Ferrer, J Switala, PC Loewen and I Fita, *J Biol Chem*, **271**, 8863–8 (1996).

35 HN Kirkman and GF Gaetani, *Proc Natl Acad Sci*, **81**, 4343–7 (1984).

36 I Fita and MG Rossmann, *Proc Natl Acad Sci*, **82**, 1604–8 (1985).

37 M Rorth and PK Jensen, *Biochim Biophys Acta*, **139**, 171–3 (1967).

38 RF Beers and IW Sizer, *J Biol Chem*, **195**, 133–8 (1952).

39 Y Maeda, A Trautwein, U Gonser, K Yoshida, K Kikuchi-Torii, T Homma and Y Ogura, *Biochim Biophys Acta*, **303**, 230–6 (1973).

40 H Theorell and A Ehrenberg, *Arch Biochem Biophys*, **41**, 442–61 (1952).

41 LK Hanson, CK Chang, MS Davis and J Fajer, *J Amer Chem Soc*, **103**, 663–70 (1981).

42 MJ Benecky, JE Frew, N Scowen, P Jones and BM Hoffman, *Biochemistry*, **32**, 11929–33 (1993).

43 MS Sevinc, MJ Mate, J Switala, I Fita and PC Loewen, *Protein Sci*, **8**, 490–8 (1999).

44 Y Ogura, *Archs Biochem Biophys*, **57**, 288–300 (1955).

45 B Chance and D Herbert, *Biochem J*, **46**, 402–14 (1950).

46 P Nicholls and GR Schonbaum, in PD Boyer (ed.), *The Enzymes*, Vol 8, Academic Press, NY, pp 147–225 (1963).

47 D Dolphin, A Forman, DC Borg, J Fajer and RH Felton, *Proc Natl Acad Sci USA*, **68**, 614–8 (1971).

48 A Ivancich, HM Jouve, B Sartor and J Gaillard, *Biochemistry*, **36**, 9356–64 (1997).

49 A Hillar and P Nicholls, *FEBS Lett*, **314**, 179–82 (1992).

50 JB Sumner and AL Dounce, *J Biol Chem*, **121**, 417–24 (1937).

51 BK Vainshtein, VR Melik-Adamyan, VV Barynin and AA Vagin, *Dokl Akad Nauk SSSR*, **250**, 242–6 (1980).

52 BK Vainshtein, WR Melik-Adamyan, VV Barynin, AA Vagin and AI Grebenko, *Nature*, **293**, 411–2 (1981).

53 MRN Murthy, TJ Reid III, A Sicignano, T Tanaka and MG Rossmann, *J Mol Biol*, **152**, 465–99 (1981).

54 TJ Reid III, MRN Murthy, A Sicignano, N Tanaka, WDL Musick and MG Rossmann, *Proc Natl Acad Sci*, **78**, 4767–71 (1981).

55 CD Putnam, AS Arvai, Y Bourne and JA Tainer, *J Mol Biol*, **296**, 295–309 (2000).

56 J Bravo, MJ Maté, T Schneider, J Switala, K Wilson, I Fita and PC Loewen, *Proteins*, **34**, 155–66 (1999).

57 GN Murshudov, WR Melik-Adamyan, AI Grebenko, VV Barynin, AA Vagin, BK Vainshtein, Z Dauter and KS Wilson, *FEBS Lett*, **312**, 127–31 (1992).

58 BK Vainshtein, WR Melik-Adamyan, VV Barynin, AA Vagin, AI Grebenko, VV Borisov, KS Bartels, I Fita and MG Rossmann, *J Mol Biol*, **188**, 49–61 (1986).

59 I Fita, AM Silva, MRN Murthy and MG Rossmann, *Acta Crystallogr. B*, **42**, 497–515 (1986).

60 MS Sevinc, J Switala, J Bravo, I Fita and PC Loewen, *Protein Eng*, **11**, 549–55 (1998).

61 I Fita and MG Rossmann, *J Mol Biol*, **185**, 21–37 (1985).

62 JJ Tanner, SC Tu, LJ Barboour, CL Barnes and KL Krause, *Protein Sci*, **8**, 17–25 (1999).

63 DC DeLuca, R Dennis and WG Smith, *Arch Biochim Biophys*, **320**, 129–34 (1995).

64 L Cattani and A Ferri, *J Biol Res-Boll Soc It Biol Sper*, **70**, 75–82 (1994).

65 A Hillar, P Nicholls, J Switala and PC Loewen, *Biochem J*, **300**, 531–9 (1994).

66 LP Olson and TC Bruice, *Biochemistry*, **34**, 7335–47 (1995).

67 DJ Bicout, MJ Field, P Gouet and HM Jouve, *Biochim Biophys Acta*, **1252**, 172–6 (1995).

68 O Almarsson, A Sinha, E Gopinath and TC Bruice, *J Am Chem Soc*, **115**, 7093–102 (1993).

69 P Gouet, HM Jouve, PA Williams, I Andersson, P Andreoletti, L Nussaume and J Hadju, *Nature Struct Biol*, **3**, 951–6 (1996).

70 E Margoliash, A Novogrodsky and A Schejter, *Biochem J*, **74**, 339–50 (1959).

71 J Bravo, I Fita, JC Ferrer, W Ens, A Hillar, J Switala and PC Loewen, *Protein Sci*, **6**, 1016–23 (1997).

72 WR Melik-Adamyan, J Bravo, J Switala, MJ Maté, I Fita and PC Loewen (submitted).

73 MJ Maté, M Serdal Sevinc, B Hu, J Bujons, J Bravo, J Switala, W Ens, PC Loewen and I Fita, *J Biol Chem*, **274**, 27717–25 (1999).

74 M Zamocky, C Herzog, LM Nykyri and F Koller, *FEBS Lett*, **367**, 241–5 (1995).

75 TL Poulos and BC Finzel, in MTW Hearn (ed.), *Peptide and Protein Reviews*, Vol 4, Marcel Dekker, New York and Bassel, pp 115–71 (1984).

76 JH Dawson, *Science*, **240**, 433–9 (1988).

77 M Zamocky, S Janecek and F Koller, *Biologia*, **52**, 723–30 (1997).

78 MK Gilso, TP Straatsma, JA McCammon, DR Ripoll, CH Faerman, PH Axelsen, I Silman and JL Sussman, *Science*, **263**, 1276–8 (1994).

79 RM Esnouf, *J of Molecular Graphics and Modelling*, **15**, 133–8 (1997).